

Study of a Multiband Rhombic Fractal Patch Antenna

Priti Sharma

*Research Scholar, Mewar University Rajasthan
Assistant Professor, Department of Computer Engineering
BITS, Noida, India*

R. L. Yadava

*Galgotias College of Engineering and Technology
Gr. Noida G. B. Nagar Uttar Pradesh, India*

Abstract Present paper describes a multi-band Rhombic Fractal Patch Antenna (RFPA), which is designed on a FR4 dielectric substrate of thickness $h = 0.8$ mm. The proposed fractal has been simulated using Ansoft HFSS (Version-14), and obtained results show that the third iterated fractal resonates at four frequencies and thus suitable for quad band applications.

I. INTRODUCTION

A **fractal antenna** is an antenna that uses a fractal, self-similar design to maximize the length, or increase the perimeter (on inside sections or the outer structure), of material that can receive or transmit electromagnetic radiation within a given total surface area or volume. Such fractal antennas are also referred to as multilevel and space filling curves, but the key aspect lies in their repetition of a motif over two or more scale sizes,^[1] or "iterations". For this reason, fractal antennas are very compact, multiband or wideband, and have useful applications in cellular telephone and microwave communications.

A good example of a fractal antenna as a spacefilling curve is in the form of a shrunken fractal helix. Here, each line of copper is just a small fraction of a wavelength. A fractal antenna's response differs markedly from traditional antenna designs, in that it is capable of operating with good-to-excellent performance at many different frequencies simultaneously. Normally standard antennas have to be "cut" for the frequency for which they are to be used—and thus the standard antennas only work well at that frequency.

This makes the fractal antenna an excellent design for wideband and multiband applications. In addition the fractal nature of the antenna shrinks its size, without the use of any components, such as inductors or capacitors [1-5].

Thus Fractal geometries reflect two common properties, space-filling and self-similarity. While the space-filling property is used for antenna size reduction the self-similarity property can be successfully applied to design multi-band fractal antennas. In particular an antenna with self-similar structures provides similar surface current distributions for different frequencies, which leads to multiband behavior [6, 7].

In the year of 2007 E. Zeni et al. designed a quad patch antenna working in E5-L1 Galileo, 2.5 and 3.5 GHz Wi-Max bands from a classical rectangular patch antenna with four resonant modes located around the required spectrum regions. The operating frequencies are obtained by perturbing the perimeter of the antenna shape according to a pre-fractal Koch-like erosion process [8].

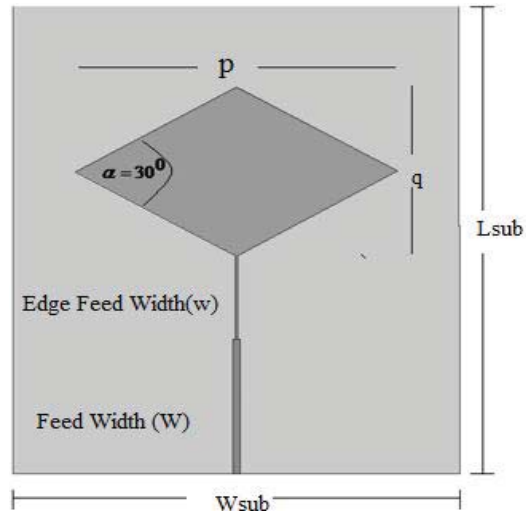


Fig.1 The geometry of the Basic Conventional rhombic antenna (Generator)

A quad-band hybrid fractal antenna designed using Koch and meander geometry in [9]. Also in [10] the author synthesized a quad-band patch antenna by shape modifications according to a fractal-shaped erosion strategy to tune the resonance frequencies and to fit the user requirements. In 2009 Renzo Azaro *et al.* designed a monopolar quad-band antenna based on a Hilbert self-affine prefractal geometry. For DCS, UMTS, LTE and ISM bands a new fractal multiband planar antenna based on elliptic geometry is presented. The quad-band slow-wave printed inverted-F antenna realized using first fractal iteration for 0.9 GHz, 1.57 GHz, 1.8 GHz, and 2.45 GHz frequencies. Multi-band behavior is achieved by combining L-loaded printed-IFA and two printed radiators [11-13]. For future wireless devices reduced physical size and multi-band capability of antenna are major design requirements

In this paper a third iterated quad band rhombic fractal patch antenna has been presented based on the Sierpinski gasket fractal geometry.

II ANTENNA GEOMETRY

Basic geometry of a rhombic antenna, shown in Fig. 1, has been designed for operation at 2.45 GHz, using fiberglass FR-4 dielectric substrate with height 0.8 mm, relative permittivity 4.4 and loss tangent 0.02. The modified dimensions of rhombic antenna are: $\alpha = 30^\circ$, $L_{sub} = 126.21$ mm, $W_{sub} = 100$ mm, $p = 36$ mm, and $q = 19$ mm. The edge feed technique is used for feed. The feed and edge feed widths are 1.53 mm and 0.36 mm respectively. Fig. 2 shows the simulated frequency response of S_{11} (in dB) of this rhombic antenna.

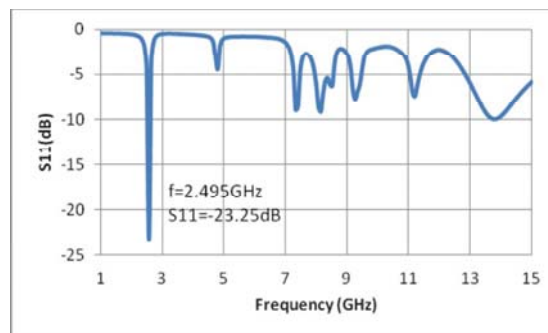
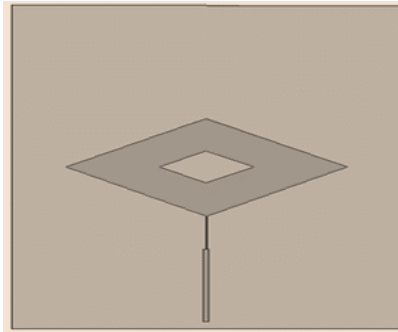


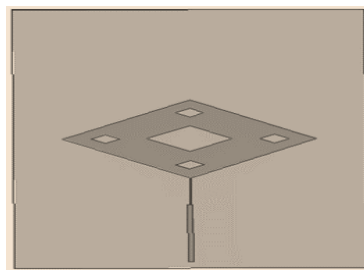
Fig. 2: Return loss (S_{11}) Vs Frequency plot of the Basic Rhombic Patch Antenna (1- 15 GHz)

The iteration steps of the Rhombic Fractal patch Antenna (RFPA) have been shown in Fig. 3. Initially the zeroth iterated fractal or the generator structure (shown in Fig. 1) has been scaled by a factor 1/3 (i.e. $p/3=12$ mm and $q/3=6.33$ mm) and subtracted from the generator in such a way that the center point of the scaled generator coincides

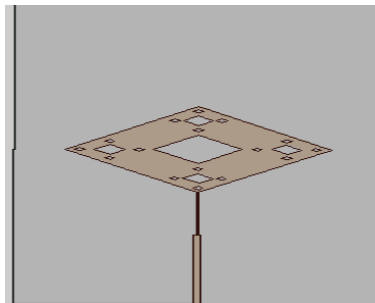
with the center point of the generator. This resulted in the 1st iterated structure, as shown in Fig. 3(a). Next, to obtain the second iterated fractal, the generator was scaled by a factor $1/9$ (i.e. $p/9= 4$ mm and $q/9=2.11$ mm) and four of such scaled generators were placed at $(\pm p/2, 0)$ and $(0, \pm q/2)$ and subtracted from the first iterated structure, as shown in Fig. 3 (b). Finally for the third iterated fractal, the generator was scaled by a factor $1/27$ (i.e. $p/27=1.33$ mm and $q/27=0.704$ mm) and sixteen of such scaled generators were placed and subtracted from the second iterated structure, as shown in Fig. 3(c). The fabricated third iterated RFPA is shown in Fig 3 (d).



(a)



(b)



(c)

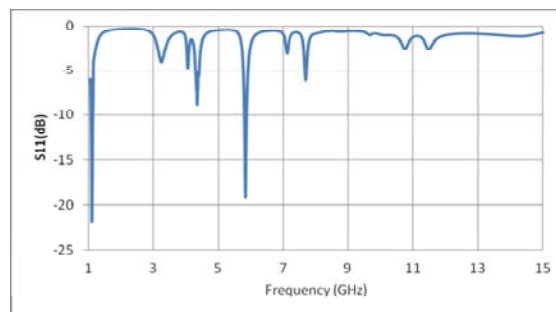


(d)

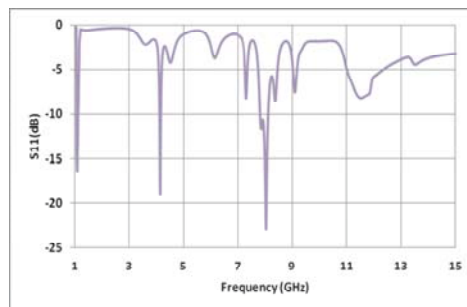
Fig. 3 Design Steps for Rhombic Fractal Patch Antenna (a) first iterated RFPA, (b) second iterated RFPA, (c) third iterated RFPA, and (d) fabricated third iterated RFPA.

III. DISCUSSIONS

The simulated frequency response of 1st and 2nd iterated fractal antennas are shown in Fig. 4. The results shows that the first iterated fractal resonates at 1.09GHz and 5.82GHz frequency bands whereas the second iterated fractal resonates at 1.084GHz,4.13GHz and 8.03GHz frequency bands respectively.



(a)Return loss (S11) vs frequency for first iterated Rhombic Fractal Patch Antenna (1-15GHz)



(b)Return loss (S11) vs frequency for Second iterated Rhombic Fractal Patch Antenna (1-15 GHz)

Fig.4 Frequency response of (a) 1st iterated fractal and (b) 2nd iterated fractal.

The fabricated third iterated RFPA has been measured using a Rohde & Schwarz Vector Network Analyzer (ZVA-40) and the measured data have been presented in Fig. 5. The simulated data also have plotted in the same figure for comparison purpose. The comparison shows that the measured result is reasonably matching with the simulated results, which validates the simulation.

Fig. 5 reveals that the simulated return loss of the third iterated RFPA is better than 10 dB at four frequencies, 1.07 GHz (1.00–1.14 GHz), 4.50 GHz (4.43–4.57 GHz), 7.51 GHz (7.44–7.58 GHz) and 13.18 GHz (12.83–13.81 GHz) with % bandwidth 13.08%, 3.11%, 1.86% and 7.443% respectively. The respective return losses are 21.00 dB, 20.24 dB, 17.52 dB and 34.84 dB. Fig. 5 also reveals that that the simulated return loss of the third iterated RFPA is better than 10 dB at four frequencies, 1.14 GHz (1.07–1.21 GHz), 4.52 GHz (4.50–4.52 GHz), 7.65 GHz (7.46–7.64 GHz) and 13.25 GHz (12.97–13.67GHz) with % bandwidth 12.33%, 0.44%, 2.35% and 5.28% respectively. The respective return losses are 14.87 dB, 14.80 dB, 13.47 dB and 21.05 dB. The slight differences between the measured and simulated results are due to fabrication constraints, uncertainties in the dielectric constant and the substrate thickness, soldering effects and the quality of the SMA connector used.

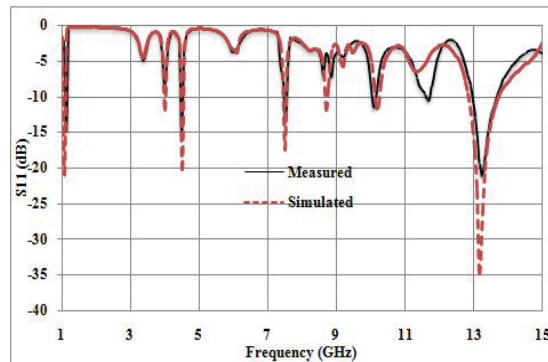
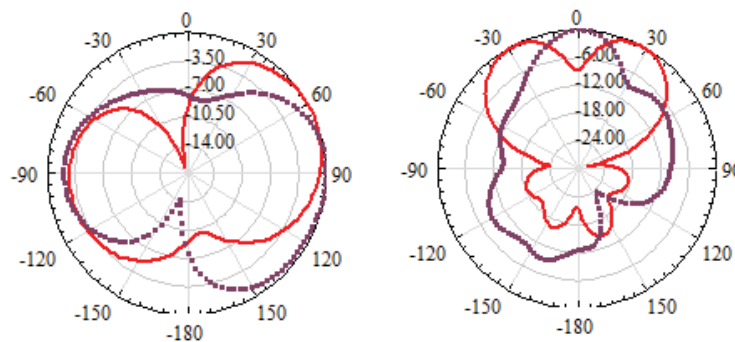


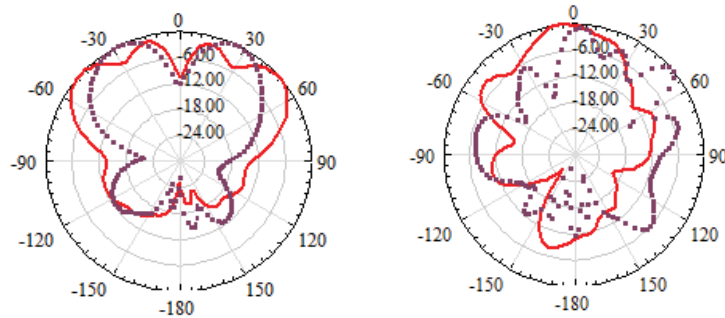
Fig.5 Comparison of simulated and measured reflection coefficient, in frequency range 1-15GHz.

The radiation patterns at all these four frequencies are shown in the Figure. In the Figure 6(a) the pattern is given for 1.07GHz frequency. The antenna gain has maximum value 2.35dB at elevation angle theta at 60 deg, when azimuthally angle phi=0 deg. The radiation is poor in the perpendicular direction (+z direction), and the antenna radiates the same ways when phi= 90deg. The radiation is about symmetrical in the xy. The reason for lower gain is due to excitation of fundamental mode of the antenna in which it behaves as first iterated rhombic fractal with removed center portion(Fig.3 a). The radiation pattern of the proposed antenna at second frequency 4.50GHz is shown in the Figure6 (b) with maximum gain of 5.29dB with directivity 6.58dB.

It is maximum when elevation angle theta= ± 25 deg at azimuthally angle phi= 0deg. At azimuthally angle phi=90deg the radiation is maximum at elevation theta=0deg(maximum radiation in the +z perpendicular direction). The pattern at the rest two frequencies 7.51 GHz & 13.18GHz are shown in the Figure6(c) & (d) with maximum gain 4.80dB & 4.75dB with directivity 6.65dB & 9.61dB respectively. From simulated data and radiation pattern it is found that the directivity increases with frequency bands i.e. fractal antenna becomes more directional with frequency bands.



(a)First Band, f=1.07GHz (b) Second Band f=4.50GHz



(c)Third Band=7.51GHz (d) Fourth Band f=13.18GHz

Fig.6 (a), (b), (c) and (d) Far-Field radiation pattern at 1.07 GHz, 4.5GHz, 7.51GHz and 13.18GHzwith $(\phi = 0^\circ \text{ \& } 90^\circ \dots\dots\dots)$

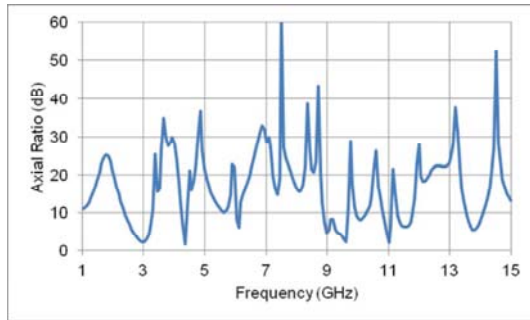
The co-polar and cross polar radiation pattern of the fractal antenna in two planes of $\phi = 0^\circ$ and $\phi = 90^\circ$ are shown in Fig. 7. The maximum far electric fields rE_{ϕ} and rE_{θ} have been plotted for each plane both co-polar and cross-polar components. In figure 7 (a) – (d) shows the co-polar (vertical) and cross-polar (horizontal) component of the far fields at 1.07GHz, 4.50GHz, 7.51GHz and 13.18GHz respectively.

The high level of cross polarization (horizontal component) seen in Fig. 7(a)-(d) justifies the presence of circularly polarized behaviour. There is a slight distortion in the radiation pattern at higher frequency due to the unequal phase distribution of the aperture electric field and increase in the magnitude of higher order modes. At all four frequencies strong co-polar components compared with cross-polar components approve elliptical or linear polarization in the structure.

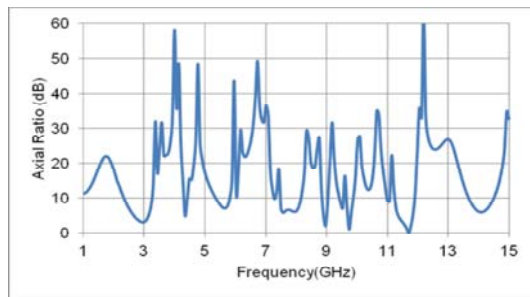
At the first frequency 1.07GHz, the maximum rE_{ϕ} is 9.04dB at $\theta = 100^\circ$ for copolar plot and 4.65dB for cross polar plot for $\phi = 0^\circ$ and $\phi = 90^\circ$ respectively. rE_{θ} is maximum 16.23dB at $\theta = 60^\circ$ for copolar plot and 13.33dB for cross polar for $\phi = 0^\circ$ and $\phi = 90^\circ$ respectively. The difference is less than 20dB which indicates non-circular polarization at first band .at the second band $f = 4.50$ GHz the maximum rE_{ϕ} is -6.287dB and 13.137dB at $\phi = 0^\circ$ and 90° respectively for rE_{θ} 21.54dB for copols and 4.07dB for cross pols at $\theta = 30^\circ$. Now for third bands $f = 7.51$ GHz the far field rE_{ϕ} is 16.81dB for copolar and -0.4968dB for cross-pol plots at $\theta = 325^\circ$ & max far field rE_{θ} 16.23dB at $\theta = 60^\circ$ for copolar and 13.33dB for cross polar for $\phi = 0^\circ$ and $\phi = 90^\circ$ respectively. For the third band the rE_{ϕ} is 16.81dB for copolar and -0.50dB for cross-polar at $\theta = 325^\circ$ deg and rE_{θ} is 21.38dB for copolar and 12.15dB for cross polar plots at $\theta = \pm 25^\circ$ deg. For $\phi = 0^\circ$ & 90° respectively. At last band frequency $f = 13.18$ GHz the far field rE_{ϕ} maximum is 18.50dB for co-polar and 3.50dB for cross polar, and rE_{θ} is 19.36dB for copolar and 0.43dB for cross polar plots at $\theta = 5^\circ$ deg respectively.

The best parameter to measure the types of polarization is Axial Ratio (AR).The AR of 1(or 1dB) is the ideal value for circularly polarization (CP) but AR less than 3 dB is an acceptable value. If AR value between 3 and 10 dB denotes elliptical polarization. In this discussion, the author has assumed wave propagation in +z direction. If the wave propagation is in -z direction, then the sense of rotation or the left- or right-handed nature of wave is reversed.Fig8 (a)- (d) illustrate the Axial Ratio(AR) variation with respect with frequencies. 1.07GHz, 4.50GHz, 7.51GHz and 13.18GHz, respectively.

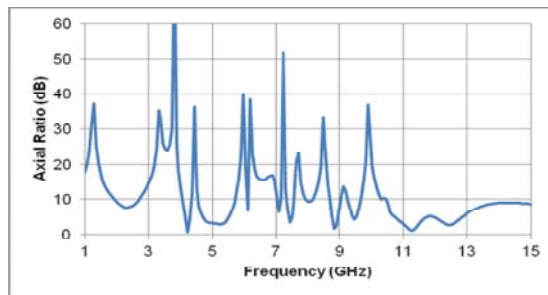
The plot for axial ratio at frequency 1.07 GHz is given in Fig. 8(a) (it is plot for copolar at $\theta = 60^\circ$ deg for $\phi = 0^\circ$ deg.) and it was found 13.86 dB which is greater than 3dB for non-circular polarization is observed. The axial ratio at frequencies 4.50GHz, 7.51GHz and 13.18GHz are 15.61dB, 4.85dB and 22.16dB respectively.



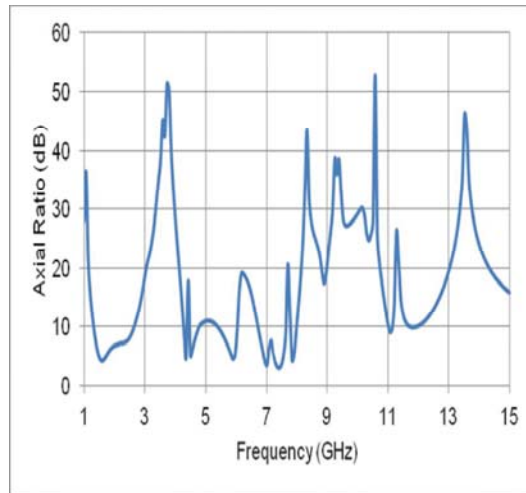
8(a) Axial Ratio vs. Frequency plot at 1.07GHz at $\theta=60\text{deg}$, $\phi=0\text{deg}$ in the frequency range 1-15GHz



(b) Axial Ratio vs. Frequency plot for 4.50GHz at $\theta=60\text{deg}$, $\phi=0\text{deg}$ in the frequency range 1-15GHz



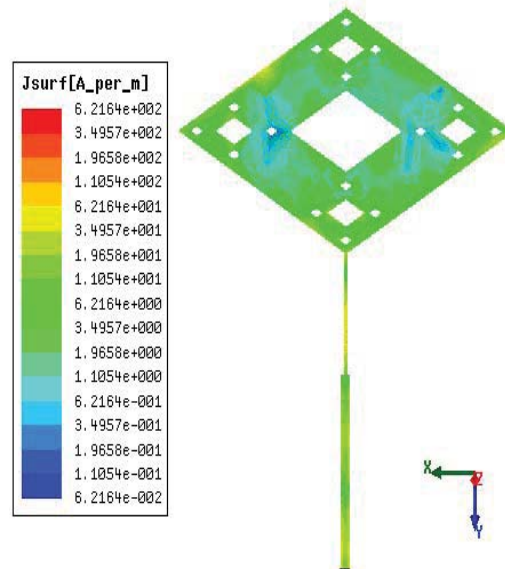
(c) Axial Ratio vs. Frequency plot for 7.51GHz at $\phi=0\text{deg}$, $\theta=30\text{deg}$ in the frequency range 1-15GHz



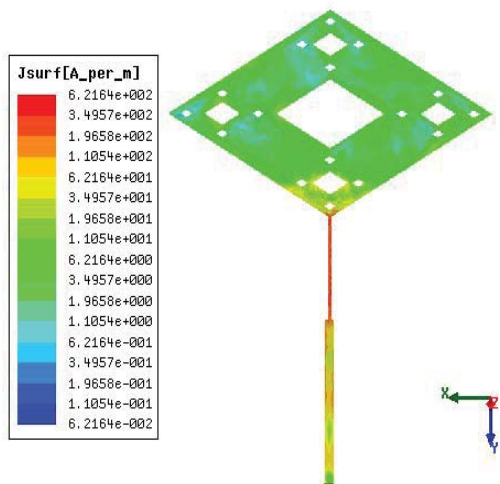
(d) Axial Ratio vs. Frequency plot for 13.18GHz at $\phi=0^\circ$ $\theta=5^\circ$ in the frequency range 1-15GHz

Fig.8. Output from Ansoft HFSSSTM: Axial Ratio vs. frequency at 1.07GHz, 4.50GHz, 7.51GHz and 13.18GHz with Azimuthally angle $\phi=0^\circ$.

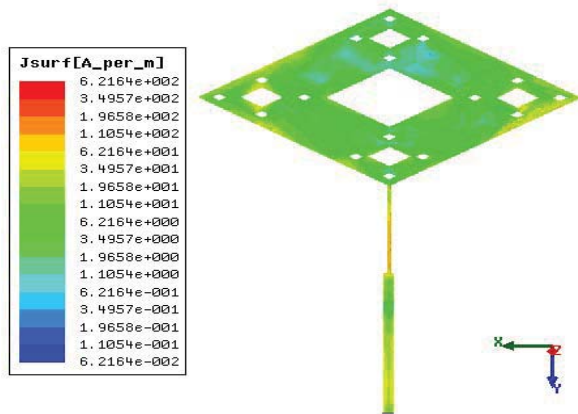
The surface current distributions of the proposed antenna, at each resonance frequencies, have been shown in Fig.9 (a)-(d). It reveals that the surface current distribution is uniform at lower resonance frequencies but becomes non-uniform at higher frequencies.



(a) First band $f=1.07\text{GHz}$



(b) First band $f=1.07\text{GHz}$



(c) Third Band $f=7.51\text{GHz}$

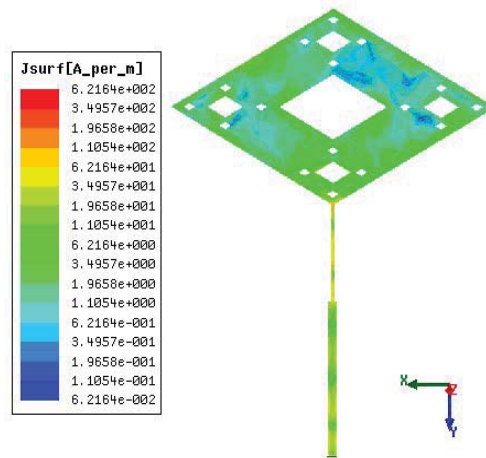
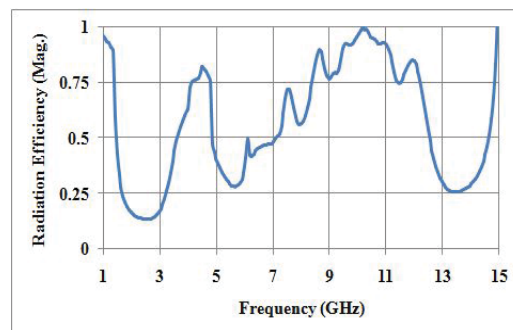
(d) Fourth band $f=13.18\text{GHz}$

Fig.9 Surface current distribution on the patch surface at (a) 1.07 GHz, (b) 4.5 GHz, (c) 7.51 GHz and (d) 13.18 GHz.

The radiation efficiency at four resonant frequencies of 1.07GHz, 4.5GHz, 7.51GHz and 13.18GHz at $\phi=0^\circ$, $\theta=0^\circ$ has been plotted in figure 10. The percentage radiation efficiencies are 94.64%, 82.29%, 71.77% and 26.87% found respectively. III.

IV. CONCLUSIONS

This paper presents a third iterated quad band rhombic shape fractal patch. The Antenna is fed with a microstrip line fed technique. The simulated results show the multiple resonances at 1.07 GHz, 4.50 GHz, 7.51 GHz, and 13.18 GHz with return losses -21.00 dB, -20.24 dB, -17.52 dB and -34.84 dB respectively. The respective frequency bands are 1.00–1.14GHz, 4.43–4.57 GHz, 7.44–7.58 GHz and 12.83–13.81GHz with % bandwidth 13.08%, 3.11%, 1.86 % and 7.443% respectively. The proposed antenna can be used for various wireless communication applications, such as, UMTS, WLAN, and Mobile WiMAX system.

Fig.10. The- Radiation Efficiency (Mag.) for $\phi=0^\circ$, $\theta=0^\circ$ at the frequencies 1.07GHz, 4.5GHz, 7.51GHz and 13.18GHz respectively

REFERENCES

- [1] J. P Gianvittorio and Y Rahmat-Sarnii, "Fractal Antenna: A Novel Antenna Miniaturization Technique and Applications", IEEE Trans. Antennas & Propagat. Vol. 44, No. 1, February 2002.
- [2] S.R. Best, "On the Significance of Self-Similar Fractal Geometry in Determining the Multiband Behavior of the Sierpinski Gasket Antenna", IEEE Antennas and Wireless Propagation Letters, Vol.1, no. 1, pp.22-25, 2002.
- [3] C.Puente, J.Romeu, R. Pous, J. Ramis and A.Hijazo, "Small but Long Koch Fractal Monopole." IEEE Electronics Letters, vol. 34, no. 1, pp. 9-10, January 1998.

- [4] Botja, C.; Romeo, I. "Multiband Sierpinski Fractal Patch Antenna" Antennas and Propagation Society International Symposium. IEEE, V01.3, pp.1708 - 1711, July 2000. 2000.
- [5] Mandelbrot, B.B. (1983): The Fractal Geometry of Nature. W.H. Freeman and Company, New York.
- [6] J. W. Harris and H. Stocker, "Scaling invariance and self-similarity and construction of self-similar objects," in Handbook of Mathematics and Computational Science. New York: Springer-Verlag, 1998, sec. 4.11.1–4.11.2, pp. 113–113.
- [7] C. Puente-Baliarda, J. Romeu, R. Pous, and A. Cardama, "On the behaviour of the Sierpinski multiband fractal antenna," IEEE Trans. Antennas Propagat., vol. 46, pp. 2340–2343, Apr. 1998.
- [8] E. Zeni, R. Azaro, P. Rocca and A. Massa, "Quad-band patch antenna for Galileo and Wi-Max services" Electronics Letters vol. 43 No. 18, 2007.
- [9] Yadwinder Kumar, Surinder Singh, "A Quad-Band Hybrid Fractal Antenna for Wireless Applications. IEEE International Advance Computing Conference pp.730-732, 2015.
- [10] P.Rocca, R. Azaro, M. Benedetti, F. Viani, E. Zeni, and A. Massa, "Multi-Band Patch Antenna Tuning by a Fractal-Shaped Erosion Process" IEEE, pp. 2008.
- [11] Renzo Azaro, Federico Viani, Leonardo Lizzi, Edoardo Zeni, and Andrea Massa, " A Monopolar Quad-Band Antenna Based on a Hilbert Self-Affine Prefractal Geometry" IEEE Antenna and wireless Propag. Letters, vol. 8, pp.177-180 2009.
- [12] T. Benyetho, J. Zbitou, L. El Abdellaoui, H. Bennis, A. Tribak, and M. Latrach, "A Novel Design of Elliptic Fractal Multiband Planar Antenna for Wireless Applications" URSI AT-RASC Conference, 2015.
- [13] Dalia M. Elsheakh and Amr M. E. Safwat, "Slow-Wave Quad-Band Printed Inverted-F Antenna" IEEE Transactions on Antennas and propagation, vol. 62, No. 8, pp.4396-4401, 2014.